and immunohistochemical analysis revealed vascular damage in the necrotic lesion, where disruption of vascular endothelial cells was indicated by fragmented $CD31^+$ marker (Fig. S1). Although the polyI:C signal is delivered by TICAM-1 and IPS-1 adaptors (11, 13), the hemorrhagic necrosis was largely alleviated in TICAM-$1^{-/-}$ mice but not in IPS-$1^{-/-}$ mice (Fig. 1*A*). The results suggest that polyI:C is a reagent that induces Lewis lung carcinoma (3LL) hemorrhagic necrosis, and the TICAM-1 pathway and its products, including TNF-α, are preferentially involved in this response.

3LL implant tumors grew well in WT C57BL6 mice. PolyI:C, when i.p. injected, resulted in tumor growth retardation (Fig. 1*B*). The retardation of tumor growth by polyI:C was also impaired in TNF-$\alpha^{-/-}$ mice (Fig. 1*B*), suggesting that TNF-α is a critical effector for not only induction of hemorrhagic necrosis but also further 3LL tumor regression. To investigate the signaling pathway involved in the tumor growth retardation by polyI:C, we challenged WT, MyD88$^{-/-}$, TICAM-$1^{-/-}$, and IPS-$1^{-/-}$ mice with 3LL implantation and then treated the mice with i.p. injection of polyI:C. 3LL growth retardation was observed in both IPS-$1^{-/-}$ (Fig. 1*C*) and MyD88$^{-/-}$ mice, to a similar extent to WT mice. In contrast, polyI:C-dependent tumor growth retardation was abrogated in TICAM-$1^{-/-}$ mice (Fig. 1*D*). The size differences of the implanted tumors became significant within 2 d after polyI:C treatment, suggesting that the molecular effector for tumor regression is induced early and its upstream is TICAM-1. Similar results were obtained with MC38 implant tumor (Fig. S2*A*), which is TNF-α sensitive and MHC class I positive (Table S1) (26).

PolyI:C is a reagent that induces natural killer (NK) cell activation in MHC class I-negative tumors (12), and 3LL cells are class I negative and NK cell sensitive (Table S1) (27, 28). We tested whether NK cells activated by polyI:C damage the 3LL tumor in mice. Tumor growth was not affected by pretreatment of the mice with anti-NK1.1 Ab in this model (Fig. S3). Thus, NK cells, at least the $NK1.1^+$ cells, have a negligible ability to retard tumor growth in vivo.

PolyI:C Induces TNF-α Through the TICAM-1 Pathway in Mice. To test whether polyI:C treatment had elicited TNF-α production in vivo, we investigated the cytokine profiles of serum from polyI:C-stimulated WT and IPS-$1^{-/-}$ and TICAM-$1^{-/-}$ mice by ELISA. Prominent differences in TNF-α levels were observed in serum collected from polyI:C-injected WT and TICAM-$1^{-/-}$ mice. Serum TNF-α levels in WT and IPS-$1^{-/-}$ mice were significantly higher than that in TICAM-$1^{-/-}$ mice within 1 h after polyI:C injection (Fig. S4 *A* and *B*). IFN-β is a main output for polyI:C stimulation (11), and its production was decreased in TICAM-$1^{-/-}$ mice and totally abrogated in IPS-$1^{-/-}$ mice (Fig. S4*C*). Taken together, the data indicate that the TICAM-1 pathway was able to sustain a high TNF-α level in the early phase of polyI:C treatment, which is independent of IPS-1 and subsequent production of IFN-β.

TICAM-1^+ Cells in Tumor Produces TNF-α in Response to PolyI:C Stimulation. Using the 3LL implant WT, IPS-$1^{-/-}$, and TICAM-$1^{-/-}$ mouse models, we tested whether polyI:C-induced early TNF-α was responsible for the lately observed tumor regression. Time-course analyses of the polyI:C-induced TNF-α protein levels were performed by ELISA using serum samples and tumors extracted from the experimental mice. The tumor TNF-α levels in WT and IPS-$1^{-/-}$ mice increased at 2 h after polyI:C i.p. injection (Fig. 2*A*). The serum TNF-α levels in both were rapidly up-regulated within 1 h after polyI:C injection, although in WT the levels continued to increase but in IPS-$1^{-/-}$ mice gradually decreased (Fig. 2*B*). In TICAM-$1^{-/-}$ mice, however, no appreciable up-regulation of TNF-α protein was detected in either tumor or serum samples during the early time-course tested. To test whether the induced TNF-α protein was generated de novo in tumors, we examined the corresponding mRNA levels in excised tumors (Fig. 2*C* and Table S2). The TNF-α mRNA levels peaked between 1 and 2 h after polyI:C injection, whereas the TNF-α protein level was kept high at >2 h after polyI:C injection in tumor as well as serum. In the TICAM-$1^{-/-}$ mice, TNF-α production was largely abrogated in the tumor and serum samples, suggesting that TNF-α was mainly produced and secreted in response to polyI:C stimulation from the TLR3/TICAM-1^+ cells within the tumor.

F4/80$^+$/Gr-1^- Mfs in 3LL Tumor Produce TNF-α Leading to Tumor Damage. We next investigated the cell types that had infiltrated the tumor by using various Mf markers in FACS analysis and tumor samples extracted at 1 h after polyI:C injection. We discovered that $CD45^+$ cells in the tumor produced TNF-α in response to polyI:C (Fig. 3*A*). The major population of those $CD45^+$ cells was determined to be of $CD11b^+$ myeloid-lineage cells that coexpressed $F4/80^+$, $Gr1^+$, or $CD11c^+$. A small population of $NK1.1^+$ cells was also detected. $CD4^+$ T cells, $CD8^+$ T cells, and B cells were rarely detected in these implant tumors (Fig. S5*A*). Moreover, $F4/80^+$/Gr-1^- cells were found to be the principal contributors to polyI:C-mediated TNF-α production (Fig. 3 *B* and *C*). $F4/80^+$ cells in 3LL tumor highly expressed macrophage mannose receptor (MMR; CD206), a M2 macrophage marker, in contrast to splenic $F4/80^+CD11b^+$ cells. Both TNF-α–producing and –nonproducing $F4/80^+$ cell populations in 3LL tumor showed indistinguishable levels of CD206 (Fig. S6), and dissimilar to MDSCs or splenic Mfs, as determined by the surface marker profiles (Table S3). Thus, the source of the TNF-α–producing cells in tumor is likely $F4/80^+$ Mfs with a TAM-like feature.

We harvested $F4/80^+$ cells from tumor samples extracted from WT and TICAM-$1^{-/-}$ mice at 30 min after polyI:C injection. These cells were used in in vitro experiments to verify the TNF-α–producing abilities and 3LL cytotoxicity properties (Fig. 4 *A* and *B*). WT $F4/80^+$ Mfs exhibited normal TNF-α–producing function and were able to kill 3LL cells upon exposure. This tumoricidal activity was ~50% neutralized by the addition of anti–TNF-α Ab (Fig. 4*C*), although incomplete inhibition by this mAb may reflect participation of other factors in TNF-α cytotoxicity. Furthermore, when active TNF-α protein (rTNF-α) was added exogenously to 3LL cell culture, the cytotoxic effects were still present and occurred in a dose-dependent manner (Fig. 4*D*). TNF-α–producing ability was also observed in $F4/80^+$ cells from implant tumor of MC38, B16D8, or EL4, and only the MC38 tumor was remediable by TICAM-1–derived TNF-α (Fig. S2 *B* and *C*). The MC38 tumor contained the $F4/80^+$/$CD11b^+$/Gr-1^- cells, as in the 3LL tumor (Fig. S5*B*).

IFN-β did not enhance rTNF-α–mediated 3LL killing efficacy (Fig. S7*A*), a finding that was consistent with previously published data (29). No effect of IRF3/7 on polyI:C-induced 3LL tumor regression in vivo was confirmed using IRF3/7 double-knockout mice. However, polyI:C-dependent tumor regression was abrogated in 3LL-bearing IFN-α/β receptor (IFNAR)$^{-/-}$ mice (Fig. S7*B*). Quantitative PCR analysis of cells from WT vs. IFNAR$^{-/-}$ tumor-bearing mice revealed that the TLR3 level was basally low and not up-regulated in response to polyI:C in tumor-infiltrating $F4/80^+$ Mfs of IFNAR$^{-/-}$ mice (Fig. S7*C*). Accordingly, the TNF-α level was not up-regulated in tumor and serum in polyI:C-stimulated IFNAR$^{-/-}$ mice (Fig. S7*D*). Thus, basal induction of type I IFN serves as a critical factor for TLR3 function in tumor $F4/80^+$ Mfs to produce TNF-α in vivo. These results suggest that the direct effector for 3LL cytolysis by polyI:C involves TNF-α, which is derived from TICAM-1 downstream independent of the IRF3/7 axis. Our results indicate that cytotoxic TNF-α is produced via a distinct route from initial type I IFN and downstream of TICAM-1 in $F4/80^+$ TAM-like Mfs. Type I IFN do not synergistically act with TNF-α on 3LL killing, but is required to complete the TLR3/TICAM-1 pathway.

These results were confirmed by in vitro assay, wherein the $F4/80^+$ Mfs harvested from 3LL tumors in WT, TICAM-$1^{-/-}$, IPS-$1^{-/-}$, and TLR3$^{-/-}$ mice were stimulated with polyI:C (Fig. S8*A*). Both TNF-α release and 3LL cytotoxic abilities of polyI:C-stimulated $F4/80^+$ Mfs were specifically abrogated by the absence of TICAM-1 and TLR3 (Fig. S8 *A* and *B*). IPS-1 or

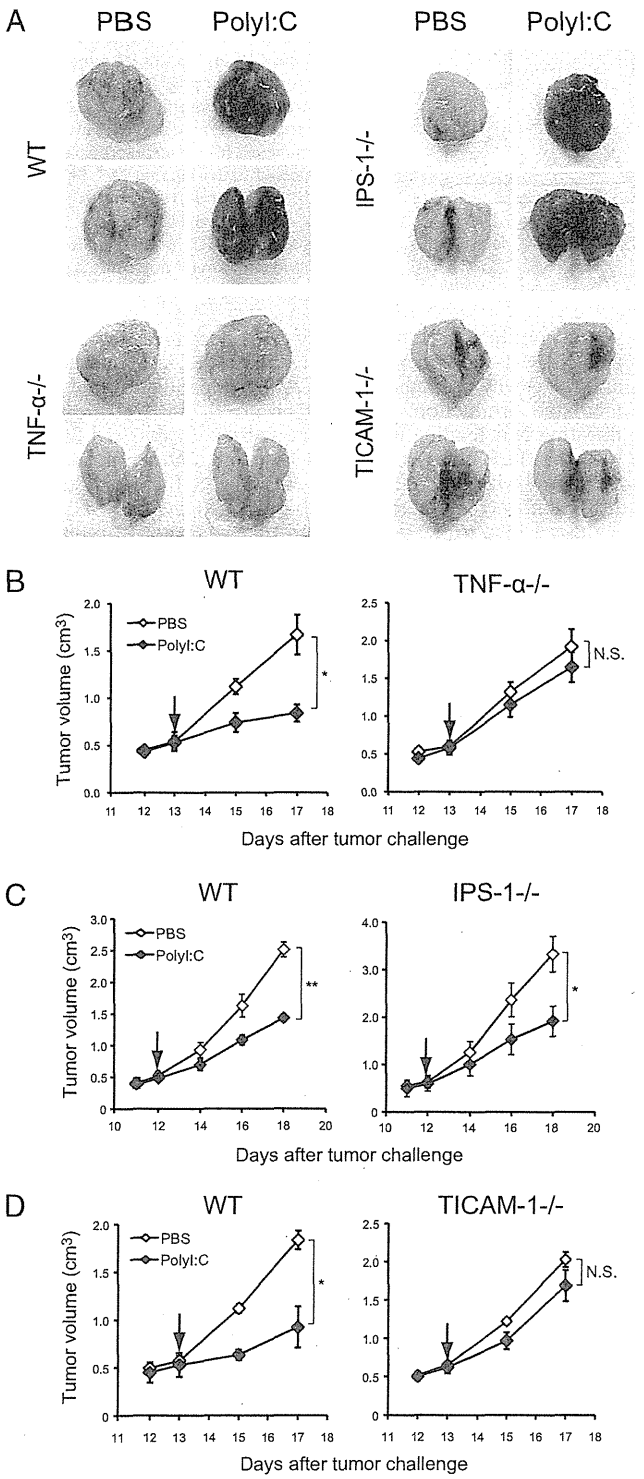

Fig. 1. Antitumor activity of polyI:C against 3LL tumor cells is mediated by the TICAM-1 pathway in vivo. (*A*) Representative photographs of 3LL tumors excised from WT, TNF-$\alpha^{-/-}$, TICAM-$1^{-/-}$, and IPS-$1^{-/-}$ mice. Whole tumor (*Upper*) and bisected tumor (*Lower*) are shown. (*B–D*) On day 0, 3LL tumor cells (3×10^6) were s.c. implanted into B6 WT (*B–D*), TNF-$\alpha^{-/-}$ (*B*), TICAM-$1^{-/-}$ (*C*), and IPS-$1^{-/-}$ (*D*) mice. PolyI:C i.p. injection was started on the day indicated by arrow, then repeated every 4 d. Data are shown as tumor average size ± SE; $n = 3$–4 mice per group. $^*P < 0.05$; $^{**}P < 0.001$. N.S., not significant. A representative experiment of two with similar outcomes is shown.

MyD88 in F4/80$^+$ Mfs had no or minimal effect on the TNF-α tumoricidal effect against 3LL tumors. PolyI:C did not directly exert a cytotoxic effect on 3LL tumor cells (Fig. S8*C*).

Role of the IPS-1 Pathway in F4/80$^+$ Cells. Both TICAM-1 and IPS-1 are known to converge their signals on transcription factors NF-κB and IRF-3, which drive expression of TNF-α and IFN-β, respectively. PolyI:C-induced TNF-α production was reduced in F4/80$^+$ cells extracted from tumors of TICAM-$1^{-/-}$ mice, but not in samples of IPS-$1^{-/-}$ mice. We examined the expression of IFN-β in these cells after polyI:C stimulation. Compared with F4/80$^+$ cells from WT mice, IFN-β expression and production was barely decreased in IPS-$1^{-/-}$ F4/80$^+$ cells, but largely impaired in TICAM-$1^{-/-}$ F4/80$^+$ cells (Fig. S9*A*) as other cytokines tested. M1 Mf-associated cytokines/chemokines were generally reduced in TICAM-$1^{-/-}$ F4/80$^+$ cells compared with WT and IPS-$1^{-/-}$ cells >4 h after polyI:C stimulation (Fig. S9*A*), whereas M2 Mf-associated genes were barely affected by TICAM-1 disruption or polyI:C stimulation (Fig. S9*B*).

Most types of Mfs are known to express TLR3 in mice (30). Messages and proteins for type I IFN induction were conserved in the F4/80$^+$ tumor-infiltrating Mfs (Fig. S10 *A–C*). However, the TLR3 mRNA level was low in macrophage colony-stimulating factor (M-CSF)–derived Mfs compared with TAMs (Fig. S10*D*). We further examined whether IFN-β production might also have relied on the TICAM-1 pathway in other types of Mfs upon stimulation with polyI:C. In contrast to the F4/80$^+$ cells isolated from tumor (Fig. S11 *A* and *B*), the IPS-1 pathway was indispensable for polyI:C-mediated IFN-β production in mouse peritoneal Mfs and M-CSF–induced bone marrow-derived Mfs (Fig. S11 *C* and *E*). However, IPS-1 only slightly participated in polyI:C-mediated TNF-α production in these Mf subsets (Fig. S11 *D* and *F*). It appears then that the IPS-1 pathway is able to signal the presence of polyI:C and subsequently induce type I IFN. TICAM-1 is the protein that induces effective TNF-α in all subsets of Mfs.

PolyI:C Influences Polarization of TAMs. Plasticity is a characteristic feature of Mfs (25). Various factors and signals can influence polarization of Mf cells to induce the M1/M2 transition, which is accompanied by a substantial change in the Mf cell's expression profile of cytokines and chemokines. Previous studies have demonstrated that Mfs that have infiltrated into tumor are of the M2-polarized phenotype, which is known to contribute to tumor progression. To test the effects of polyI:C on the polarization of tumor-infiltrated Mf cells, we analyzed the gene expression profiles of these cells following in vitro polyI:C stimulation, and representative profiles were confirmed by quantitative PCR (Fig. 5 *A* and *B*). The mRNA expressions were increased for M1 Mf markers IL-12p40, IL-6, CXCL11, and IL-1β at 4 h after in vitro polyI:C treatment, as were mRNA levels of IFN-β and TNF-α and ex vivo results. The M2 Mf markers arginase-1 (*Arg1*), chitinase 3-like 3 (*Chi3l3*), and MMR (*Mrc1*) were unchanged, compared with unstimulated levels; however, the M2 Mf marker IL-10, a regulatory cytokine, was induced. In addition, there was no difference observed in the mRNA expression levels of MMP9 (*Mmp9*) and VEGFA (*Vegfa*), both of which are involved in tissue remodeling and angiogenesis events of tumor progression (Fig. 5*C*). The polyI:C-induced M1 markers and IL-10 expression that were up-regulated in WT and IPS-$1^{-/-}$ F4/80$^+$ cells were found to be abrogated in TICAM-$1^{-/-}$ F4/80$^+$ cells (Fig. 5 *A* and *B*), reinforcing the results obtained with F4/80$^+$ Mfs isolated from 3LL tumors in mice injected with polyI:C (Fig. S9 *A* and *B*). It appears that TICAM-1 is responsible for the M1 polarization of F4/80$^+$ Mf cells in tumors, but has no effect on M2 markers. We further examined the expression of IRF-5 and IRF-4, which are considered the master regulators for M1 and M2 polarization, respectively (31, 32). As expected, polyI:C induced IRF-5 mRNA expression, but had no effect on IRF-4 mRNA expression in vitro (Fig. 5 *A* and *B*). Jmjd3, a histone H3K27 demethylase involved in IRF-4 expression, is reportedly induced by TLR stimulation (33). In our study, polyI:C stimulation increased Jmjd3 mRNA in F4/80$^+$ cells

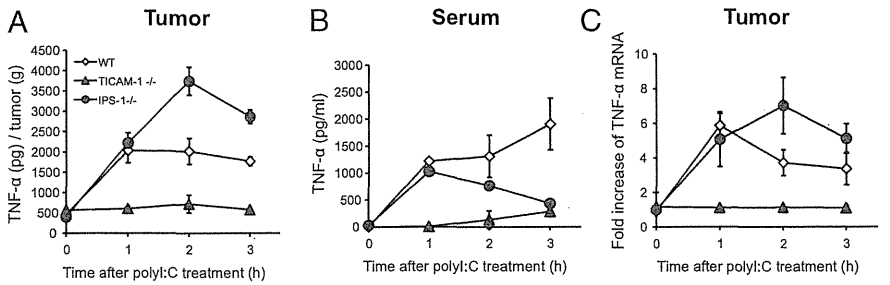

Fig. 2. TNF-α production in tumor and serum of polyI:C-injected 3LL tumor-bearing mice. Mice bearing 3LL tumor were i.p. injected with 200 μg polyI:C. Tumor (*A*) and serum (*B*) were collected at 0, 1, 2, and 3 h after polyI:C injection, and TNF-α concentration was determined by ELISA. TNF-α level in tumor is presented as [TNF-α protein (pg)/tumor weight (g)]. (*C*) Tumors were isolated from polyI:C-injected tumor-bearing WT, TICAM-1$^{-/-}$, and IPS-1$^{-/-}$ mice, and TNF-α mRNA was measured by quantitative PCR; n = 3. Data are shown as average ± SD. A representative experiment of two with similar outcomes is shown.

(Fig. 5*B*). The polyI:C-triggered M1 gene expression continued long in tumor-infiltrated Mfs, a finding that may further explain the tumor-suppressing feature of these Mfs, in addition to the concern of early inducing TNF-α.

Discussion

In this study we demonstrated that the tumor-supporting properties of tumor-infiltrating F4/80$^+$ Mfs characterized by M2 markers are dynamic and able to shift to an M1-dominant state upon the particular signal provided by PRRs. In 3LL tumors that express minimal amounts of MHC class I/II and recruit a large amount of myeloid cells, F4/80$^+$ Mfs function to sustain the tumor in the surrounding microenvironment. This tumor-supporting environment can be disrupted by stimulation with an RNA duplex through a TICAM-1 signal and subsequent induction of mediators such as TNF-α. Thus, the TICAM-1 signal in tumor-infiltrating Mfs plays a key role in TNF-α and M1 shift-mediated tumor regression. These results were confirmed using another cell line, MC38 colon adenocarcinoma (34), although MC38 cells express MHC class I. B16D8 melanoma (12) and EL4 lymphoma (35) were resistant to TNF-α, but their F4/80$^+$ Mfs still possessed TNF-α–inducing potential by stimulation with polyI:C; their susceptibilities to polyI:C reportedly depend on other effectors (12, 35). These results may partly explain the reported findings that tumors regressed in patients with simultaneous virus infection (36, 37), and that tumor growth was inhibited by polyI:C injection in tumor-bearing mice (6, 7).

In contrast, polyI:C-stimulated PEC or bone marrow-derived Mfs induce type I IFN via the IPS-1 pathway unlike the case of tumor-infiltrating F4/80$^+$ Mfs. Nevertheless, all of these Mf subsets produce proinflammatory cytokines, including TNF-α, in a TICAM-1–dependent manner. Thus, the key question that arose was why predominant TICAM-1 dependence for polyI:C-mediated production of TNF-α occurred in F4/80$^+$ tumor-infiltrating Mfs leading to tumor regression. A marked finding is that the TLR3 protein level is high in tumor-infiltrating Mfs compared with other sources of Mfs (Fig. S10). In addition, the IPS-1 pathway is unresponsive to polyI:C if the polyI:C is exogenously added to the tumor-infiltrating Mfs without transfection reagents. The cytoplasmic dsRNA sensors normally work for IFN induction in tumor F4/80$^+$ Mfs if the polyI:C is transfected into the cells. TICAM-1–dependent TNF-α production by F4/80$^+$ Mfs (Fig. S11 *D* and *F*) occurs partly because F4/80$^+$ Mfs express a high basal level of TLR3 and fail to take up extrinsic polyI:C into the cytoplasm. Of many subsets of Mfs, these properties (38) are unique to the F4/80$^+$ Mfs.

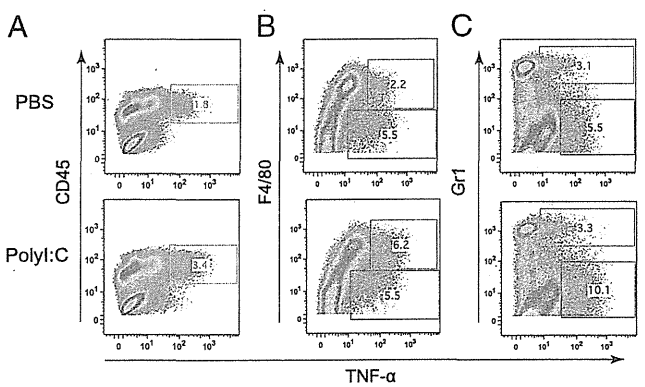

Fig. 3. F4/80$^+$ cells are responsible for the polyI:C-induced elevation of TNF-α production in tumor. Mice bearing 3LL tumors were i.p. injected with 200 μg polyI:C. TNF-α–producing cells in tumors of polyI:C- or PBS-injected mice were examined by immunohistochemical staining and flow cytometry to determine intracellular cytokine expression profiles of CD45$^+$ cells (*A*), F4/80$^+$ cells (*B*), and Gr1$^+$ cells (*C*). CD45$^+$ cells in tumor were gated and are shown in *B* and *C*. A representative experiment of two with similar outcomes is shown. TNF-α$^+$ gating squares are shown in red (positive) and green (negative).

Hemorrhagic necrosis and tumor size reduction are closely correlated with constitutive production of TNF-α (39, 40). The association of PRR-derived TNF-α and hemorrhagic necrosis of tumor has been described earlier. Carswell et al. (41) showed that TNF-α is robustly expressed in mouse serum following treatment with bacillus Calmette–Guérin and endotoxin. Bioassay of TNF-α as reflected by the degree of hemorrhagic necrosis of transplanted Meth A sarcoma in BALB/c mice led the authors to speculate that Mfs are responsible for TNF-α induction. Many years later, Dougherty et al. (42) identified the mechanism responsible for the TNF-α production associated with antitumor activity; macrophages isolated from tumors in mice with inactivating mutation in the TLR4 gene [Lps(d) in C3H/HeJ] expressed 5- to 10-fold less TNF-α than tumors in WT mice. This finding represents a unique recognition of a PRR contributing to the cancer phenotype. Subsequent studies determined that MyD88 is involved in the induction of TNF-α via TLR4 binding to its cognate ligand, lipid A endotoxin (15, 43). Because the TLR3 signal is independent of MyD88, this MyD88 concept is not applicable to the present study on polyI:C-dependent tumor regression.

Alternatively, endotoxin/lipid A may have activated TICAM-1 in previous reports on TLR4-derived TNF-α because TLR4 can recruit TICAM-1 in addition to MyD88 (15). The lipid A derivative monophospholipid A preferentially activates the TICAM-1 pathway of TLR4 (43). It is likely that TICAM-1 participates in TLR4-mediated tumor regression in addition to MyD88, although MyD88 is not involved in the polyI:C signaling. This point was further proven using TNF-α$^{-/-}$ mice: TICAM-1–derived TNF-α in F4/80$^+$ Mf cells has a critical role in the induction of tumor necrosis and regression by polyI:C. The results are consistent with the finding that both TICAM-1 and IPS-1 pathways are able to induce NF-κB activation secondary to polyI:C stimulation, and indeed their signals converge at the IκB kinase complex (18).

TICAM-1 is able to induce many of the IFN-inducible genes that MyD88 cannot in mDCs (44). In both cases of TICAM-1 and MyD88 stimulation, tumor-infiltrating Mfs facilitate the expression of many genes in addition to TNF-α. The M2 phenotype of F4/80$^+$ Mfs or tumor-associated Mfs is modified dependent on these additional factors. IFNAR facilitates polyI:C-mediated tumor regression in tumor-bearing mice, lack of which results in no induction of TLR3 (Fig. S7). Thus, preceding the polyI:C

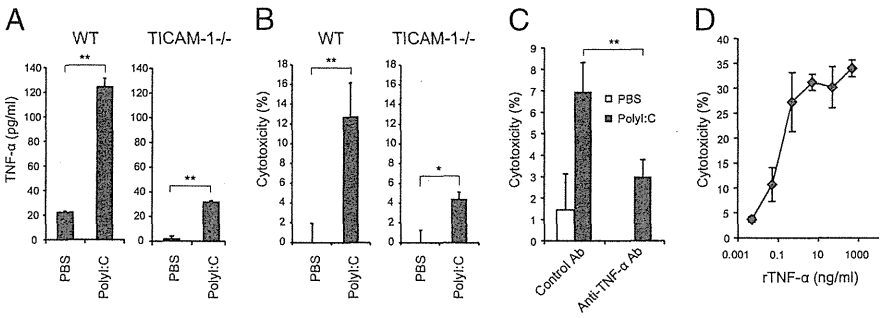

Fig. 4. PolyI:C enhances TNF-α production and cytotoxicity of F4/80$^+$ cells in tumor. PolyI:C (200 μg) or PBS was i.p. injected into 3LL tumor-bearing WT mice. After 30 min, F4/80$^+$ cells isolated from tumor were cultured for 24 h and TNF-α concentration in the conditioned medium was determined by ELISA (*A*). In parallel, the cytotoxicity of tumor-infiltrating F4/80$^+$ cells against 3LL tumor cells was measured by ^{51}Cr-release assay (*B*). Anti–TNF-α neutralization antibody or control antibody was added (10 μg/mL) to mixed culture of isolated tumor-infiltrating F4/80$^+$ cells and 3LL tumor cells (*C*). (*D*) Cytotoxic activity of TNF-α against 3LL tumor cells. Recombinant TNF-α was added to ^{51}Cr-labeled 3LL tumor cell culture at various concentrations. After 20 h, cytotoxicity was measured; $n = 3$. Data are shown as average ± SD. $*P < 0.05$, $**P < 0.001$. A representative experiment of three with similar outcomes is shown.

response, minute type I IFN of undefined source has to be provided to set the TLR3/TICAM-1 pathway, which may primarily fail in IFNAR$^{-/-}$ mice. Cellular effectors, cytotoxic T lymphocyte (CTL) and NK cells, are induced secondary to activation of IFN-inducible genes in a late phase of polyI:C-stimulated myeloid cells (45–47). The relationship among the TICAM-1–mediated type I IFN liberation, these late-phase effectors, and tumor regression remains an open question in this setting.

M1 Mf cells function to protect the host against tumors by producing large amounts of inflammatory cytokines and activating the immune response (48, 49). However, distinct types of M2 cells differentiate when monocytes are stimulated with IL-4 and IL-13 (M2a), immune complexes/TLR ligands (M2b), or IL-10 and glucocorticoids (M2c) (50). In our study, polyI:C stimulation led to incremental expression of the M1 Mf-related genes. In contrast, polyI:C stimulation was not associated with M2 polarization, except for IL-10. Other genes related to angiogenesis and extravasation were not affected by polyI:C treatment. Thus, polyI:C was able to induce the characteristic M1 conversion and, in turn, contribute to tumor regression. It is notable that TAM cells usually have defective and delayed NF-κB activation in response to different proinflammatory signals, such as expression of cytotoxic mediators NO, cytokines, TNF-α, and IL-12 (51–53). These observations are in apparent contrast with the function of other resident Mf species. This discrepancy may again reflect a dynamic change in the tumor microenvironment during tumor progression.

In line with our findings, virus infection has been observed to instigate tumor regression in patients with cancer (36, 54). Gene therapy for cancer patients using virus-derived vectors has proved effective in reducing tumors in clinic (36, 37). Administration of dsRNA elicits IFN induction, NK cell activation, and CTL proliferation for antitumor effectors in vivo (19, 55). This is a unique finding that tumor-infiltrating Mfs are a target of dsRNA and converted from tumor supporters to tumoricidal effectors. Hence, the antitumor effect of dsRNA adjuvant is ultimately based on the liberation of type I IFN, functional maturation of mDCs, and modulation of tumor-infiltrating Mfs, where TICAM-1 is a crucial transducer in eliciting antitumor immunity.

Methods

Inbred C57BL/6 WT mice were purchased from CLEA Japan, Inc. TICAM-1$^{-/-}$ and IPS-1$^{-/-}$ mice were generated in our laboratory and maintained as described previously. IRF-3/7 double-KO mice were a gift from T. Taniguchi

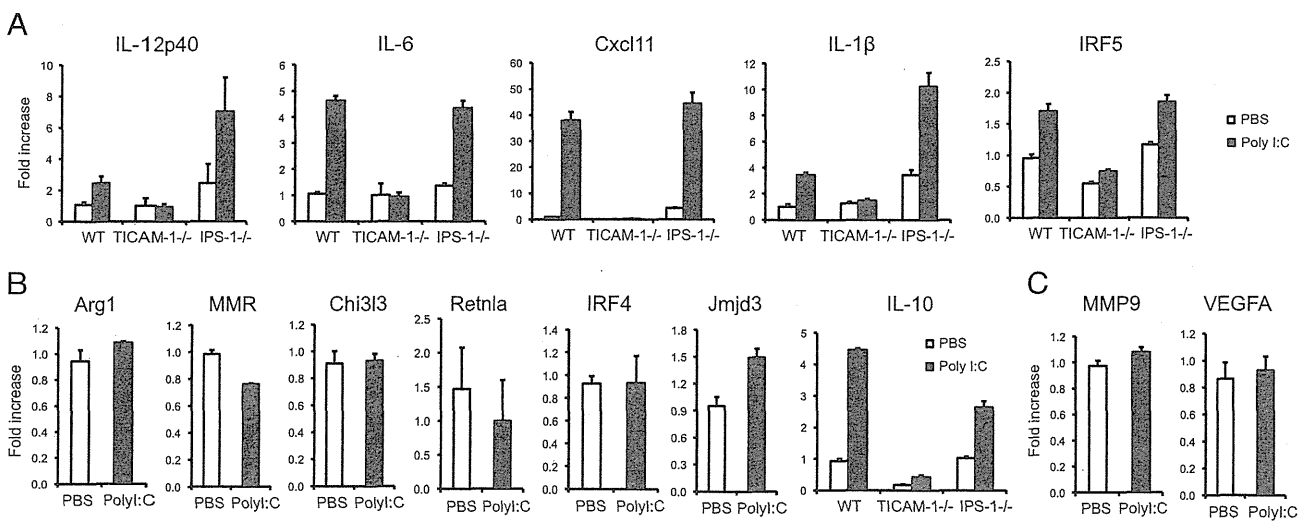

Fig. 5. PolyI:C induces M1 polarization of TAMs. F4/80$^+$ cells were isolated from 3LL tumor and stimulated with polyI:C (50 μg/mL) for 4 h. Total RNA was extracted and used to analyze the transcript expression levels of M1 (*A*) and M2 (*B* and *C*) markers; $n = 3$. Data are shown as average ± SD. A representative experiment of two with similar outcomes is shown.

(University of Tokyo, Tokyo, Japan). TNF-$\alpha^{-/-}$ mice were kindly provided by A. Nakane (Hirosaki University, Aomori, Japan) and Y. Iwakura (University of Tokyo). Mice 6–10 wk of age were used in all experiments. 3LL lung cancer cells were cultured at 37 °C under 5% CO_2 in RPMI containing 10% FCS, penicillin, and streptomycin. This study was carried out in strict accordance with the recommendations in the Guide for the Care and Use of Laboratory Animals of the National Institutes of Health. The protocol was approved by the Committee on the Ethics of Animal Experiments in the Animal Safety Center, Hokkaido University, Japan. All mice were used according to the guidelines of the Institutional Animal Care and Use Committee of Hokkaido University, who approved this study as no. 08-0290, "Analysis of Anti-Tumor Immune Response Induced by the Activation of Innate Immunity."

Other detailed methods are provided in *SI Methods*.

ACKNOWLEDGMENTS. We thank Dr. T. Taniguchi (University of Tokyo) and D. M. Segal (EIB/NCI, Bethesda, MD) for kindly providing us with IRF-3/7 double KO mice and mAb against mouse TLR3. This work was supported in part by Grants-in-Aid from the Ministry of Education, Science, and Culture (MEXT), "the Carcinogenic Spiral" a MEXT Grant-in-Project, and the Ministry of Health, Labor, and Welfare of Japan, the Takeda Foundation, the Akiyama Foundation, and the Waxman Foundation.

1. Grivennikov SI, Greten FR, Karin M (2010) Immunity, inflammation, and cancer. *Cell* 140:883–899.
2. de Visser KE, Eichten A, Coussens LM (2006) Paradoxical roles of the immune system during cancer development. *Nat Rev Cancer* 6:24–37.
3. Chan AT, Ogino S, Fuchs CS (2007) Aspirin and the risk of colorectal cancer in relation to the expression of COX-2. *N Engl J Med* 356:2131–2142.
4. Rakoff-Nahoum S, Medzhitov R (2007) Regulation of spontaneous intestinal tumorigenesis through the adaptor protein MyD88. *Science* 317:124–127.
5. Chen GY, Shaw MH, Redondo G, Núñez G (2008) The innate immune receptor Nod1 protects the intestine from inflammation-induced tumorigenesis. *Cancer Res* 68: 10060–10067.
6. Sarma PS, Shiu G, Neubauer RH, Baron S, Huebner RJ (1969) Virus-induced sarcoma of mice: Inhibition by a synthetic polyribonucleotide complex. *Proc Natl Acad Sci USA* 62: 1046–1051.
7. Levy HB, Law LW, Rabson AS (1969) Inhibition of tumor growth by polyinosinic-polycytidylic acid. *Proc Natl Acad Sci USA* 62:357–361.
8. Absher M, Stinebring WR (1969) Toxic properties of a synthetic double-stranded RNA. Endotoxin-like properties of poly I. poly C, an interferon stimulator. *Nature* 223: 715–717.
9. Talmadge JE, et al. (1985) Immunomodulatory effects in mice of polyinosinic-polycytidylic acid complexed with poly-L-lysine and carboxymethylcellulose. *Cancer Res* 45: 1058–1065.
10. Longhi MP, et al. (2009) Dendritic cells require a systemic type I interferon response to mature and induce $CD4^+$ Th1 immunity with poly IC as adjuvant. *J Exp Med* 206: 1589–1602.
11. Matsumoto M, Seya T (2008) TLR3: Interferon induction by double-stranded RNA including poly(I:C). *Adv Drug Deliv Rev* 60:805–812.
12. Akazawa T, et al. (2007) Antitumor NK activation induced by the Toll-like receptor 3-TICAM-1 (TRIF) pathway in myeloid dendritic cells. *Proc Natl Acad Sci USA* 104: 252–257.
13. Miyake T, et al. (2009) Poly I:C-induced activation of NK cells by CD8 alpha$^+$ dendritic cells via the IPS-1 and TRIF-dependent pathways. *J Immunol* 183:2522–2528.
14. McCartney S, et al. (2009) Distinct and complementary functions of MDA5 and TLR3 in poly(I:C)-mediated activation of mouse NK cells. *J Exp Med* 206:2967–2976.
15. Oshiumi H, Matsumoto M, Funami K, Akazawa T, Seya T (2003) TICAM-1, an adaptor molecule that participates in Toll-like receptor 3-mediated interferon-beta induction. *Nat Immunol* 4:161–167.
16. Yoneyama M, et al. (2005) Shared and unique functions of the DExD/H-box helicases RIG-I, MDA5, and LGP2 in antiviral innate immunity. *J Immunol* 175:2851–2858.
17. Takeuchi O, Akira S (2010) Pattern recognition receptors and inflammation. *Cell* 140: 805–820.
18. Sasai M, et al. (2006) NAK-associated protein 1 participates in both the TLR3 and the cytoplasmic pathways in type I IFN induction. *J Immunol* 177:8676–8683.
19. Seya T, Matsumoto M (2009) The extrinsic RNA-sensing pathway for adjuvant immunotherapy of cancer. *Cancer Immunol Immunother* 58:1175–1184.
20. Iwasaki A, Medzhitov R (2010) Regulation of adaptive immunity by the innate immune system. *Science* 327:291–295.
21. Condeelis J, Pollard JW (2006) Macrophages: Obligate partners for tumor cell migration, invasion, and metastasis. *Cell* 124:263–266.
22. Schuler G, Schuler-Thurner B, Steinman RM (2003) The use of dendritic cells in cancer immunotherapy. *Curr Opin Immunol* 15:138–147.
23. Murdoch C, Muthana M, Coffelt SB, Lewis CE (2008) The role of myeloid cells in the promotion of tumour angiogenesis. *Nat Rev Cancer* 8:618–631.
24. Borrello MG, Degl'Innocenti D, Pierotti MA (2008) Inflammation and cancer: The oncogene-driven connection. *Cancer Lett* 267:262–270.
25. Biswas SK, Mantovani A (2010) Macrophage plasticity and interaction with lymphocyte subsets: Cancer as a paradigm. *Nat Immunol* 11:889–896.
26. Farma JM, et al. (2007) Direct evidence for rapid and selective induction of tumor neovascular permeability by tumor necrosis factor and a novel derivative, colloidal gold bound tumor necrosis factor. *Int J Cancer* 120:2474–2480.
27. Masuda H, et al. (2002) High levels of RAE-1 isoforms on mouse tumor cell lines assessed by the anti-pan-Rae-1 polyclonal antibody confers tumor cell cytotoxicity on mouse NK cells. *Biochem Biophys Res Commun* 290:140–145.
28. Smyth MJ, et al. (2004) NKG2D recognition and perforin effector function mediate effective cytokine immunotherapy of cancer. *J Exp Med* 200:1325–1335.
29. Remels L, Fransen L, Huygen K, De Baetselier P (1990) Poly I:C activated macrophages are tumoricidal for TNF-α-resistant 3LL tumor cells. *J Immunol* 144:4477–4486.
30. Jelinek I, et al. (2011) TLR3-specific double-stranded RNA oligonucleotide adjuvants induce dendritic cell cross-presentation, CTL responses, and antiviral protection. *J Immunol* 186:2422–2429.
31. Krausgruber T, et al. (2011) IRF5 promotes inflammatory macrophage polarization and TH1-TH17 responses. *Nat Immunol* 12:231–238.
32. Satoh T, et al. (2010) The Jmjd3-*Irf4* axis regulates M2 macrophage polarization and host responses against helminth infection. *Nat Immunol* 11:936–944.
33. De Santa F, et al. (2007) The histone H3 lysine-27 demethylase Jmjd3 links inflammation to inhibition of polycomb-mediated gene silencing. *Cell* 130:1083–1094.
34. Zitvogel L, et al. (1995) Cancer immunotherapy of established tumors with IL-12. Effective delivery by genetically engineered fibroblasts. *J Immunol* 155:1393–1403.
35. Abe R, Peng T, Sailors J, Bucala R, Metz CN (2001) Regulation of the CTL response by macrophage migration inhibitory factor. *J Immunol* 166:747–753.
36. Russell SJ (2002) RNA viruses as virotherapy agents. *Cancer Gene Ther* 9:961–966.
37. Aghi M, Martuza RL (2005) Oncolytic viral therapies—the clinical experience. *Oncogene* 24:7802–7816.
38. Watanabe A, et al. (2011) Raftlin is involved in the nucleocapture complex to induce poly(I:C)-mediated TLR3 activation. *J Biol Chem* 286:10702–10711.
39. Mocellin S, Rossi CR, Pilati P, Nitti D (2005) Tumor necrosis factor, cancer and anticancer therapy. *Cytokine Growth Factor Rev* 16:35–53.
40. Balkwill F (2009) Tumour necrosis factor and cancer. *Nat Rev Cancer* 9:361–371.
41. Carswell EA, et al. (1975) An endotoxin-induced serum factor that causes necrosis of tumors. *Proc Natl Acad Sci USA* 72:3666–3670.
42. Dougherty ST, Eaves CJ, McBride WH, Dougherty GJ (1997) Molecular mechanisms regulating TNF-alpha production by tumor-associated macrophages. *Cancer Lett* 111: 27–37.
43. Mata-Haro V, et al. (2007) The vaccine adjuvant monophosphoryl lipid A as a TRIF-biased agonist of TLR4. *Science* 316:1628–1632.
44. Ebihara T, et al. (2010) Identification of a polyI:C-inducible membrane protein that participates in dendritic cell-mediated natural killer cell activation. *J Exp Med* 207: 2675–2687.
45. Akazawa T, et al. (2004) Adjuvant-mediated tumor regression and tumor-specific cytotoxic response are impaired in MyD88-deficient mice. *Cancer Res* 64:757–764.
46. Akazawa T, et al. (2007) Tumor immunotherapy using bone marrow-derived dendritic cells overexpressing Toll-like receptor adaptors. *FEBS Lett* 581:3334–3340.
47. Schulz O, et al. (2005) Toll-like receptor 3 promotes cross-priming to virus-infected cells. *Nature* 433:887–892.
48. Mantovani A, Sica A, Locati M (2007) New vistas on macrophage differentiation and activation. *Eur J Immunol* 37:14–16.
49. Martinez FO, Helming L, Gordon S (2009) Alternative activation of macrophages: An immunologic functional perspective. *Annu Rev Immunol* 27:451–483.
50. Mantovani A, et al. (2004) The chemokine system in diverse forms of macrophage activation and polarization. *Trends Immunol* 25:677–686.
51. Sica A, et al. (2000) Autocrine production of IL-10 mediates defective IL-12 production and NF-kappa B activation in tumor-associated macrophages. *J Immunol* 164:762–767.
52. Torroella-Kouri M, et al. (2005) Diminished expression of transcription factors nuclear factor kappaB and CCAAT/enhancer binding protein underlies a novel tumor evasion mechanism affecting macrophages of mammary tumor-bearing mice. *Cancer Res* 65: 10578–10584.
53. Biswas SK, et al. (2006) A distinct and unique transcriptional program expressed by tumor-associated macrophages (defective NF-kappaB and enhanced IRF-3/STAT1 activation). *Blood* 107:2112–2122.
54. Bluming AZ, Ziegler JL (1971) Regression of Burkitt's lymphoma in association with measles infection. *Lancet* 2:105–106.
55. Matsumoto M, Oshiumi H, Seya T (2011) Antiviral responses induced by the TLR3 pathway. *Rev Med Virol* 21:67–77.

Supporting Information

Shime et al. 10.1073/pnas.1113099109

SI Methods

Reagents. PolyI:C was purchased from GE Healthcare, which was free from LPS contamination. TNF-α and IFN-β ELISA kit was purchased from eBioscience and PBL InterferonSource, respectively. Recombinant TNF-α was purchased from R&D Systems.

Tumor Cells and Tumor-Infiltrated Immune Cells. We first tested the amounts of macrophages (Mfs) in implant tumors formed in B6 mice. Mouse lymphoma (EL4), Lewis lung carcinoma (3LL), adenocarcinoma MC38, and melanoma (B16D8) lines grew well in the back of mice, and the Mf content was maximal in the 3LL tumor. MC38, a murine colon adenocarcinoma cell line, was a gift from S. A. Rosenberg (National Cancer Institute, Bethesda) (1). Hemorrhagic necrosis shown in Fig. 1*A* was typically induced in response to polyI:C in 3LL tumor. We then used the 3LL line for this study.

3LL cells were found to express very low amounts of detectable MHC class I or class II (Table S1), suggesting this cell type as a possible target for natural killer (NK) cells but not cytotoxic T lymphocytes (CTLs). 3LL cells were found to express appreciable amounts of the NKG2D ligand, retinoic acid-inducible gene 1, consistent with previous reports (Table S1) (2, 3). 3LL cells also expressed mRNA transcripts for Toll-like receptor 3 (TLR3), Toll–IL-1 receptor domain-containing adaptor molecule 1 (TICAM-1), IFN-β promoter stimulator 1 (IPS-1), and melanoma differentiation-associated protein 5 (MDA5). Exposure to polyI:C-stimulated peritoneal Mfs caused significant death of 3LL cells, which was likely an effect of liberated inflammatory cytokines such as TNF-α (4). Consistent with previously reported data about 3LL properties in vitro, the 3LL cells we used were not damaged by direct polyI:C treatment or exposure to 3LL-derived cytokines (Fig. S8*C*). When 3LL cells were implanted s.c. in mice, the resulting tumors were found to contain a high amount (>30%) of $CD45.2^+$ cells (Fig. S5*A*). The major population of those $CD45.2^+$ cells was determined to be of $CD11b^+$ myeloid lineage cells that coexpressed $F4/80^+$, $Gr1^+$, or $CD11c^+$. A small population of $NK1.1^+$ cells was also detected. $CD4^+$ T cells, $CD8^+$ T cells, and B cells were rarely detected in these implant tumors (Fig. S5*A*).

Cytotoxic Activity Assay. Mice bearing 3LL tumor were injected i.p. with polyI:C. Mice were killed and $F4/80^+$ cells were isolated from tumor by using MACS-positive selection beads (Miltenyi) as described previously. 3LL cells were labeled with ^{51}Cr for 3–5 h and then washed three times with the medium. $F4/80^+$ cells, and 3LL cells were cocultured at the indicated ratio. After 20 h, supernatants were harvested and ^{51}Cr release was measured in each sample. Specific lysis was calculated by the following formula: cytotoxicity (%) = [(experimental release − spontaneous release)/(max release − spontaneous release)] × 100.

Flow Cytometric Analysis. Mononuclear cells prepared from spleen and tumor were treated with anti-CD16/32 (no. 93) and stained with APC–anti-CD45.2 (no. 104), FITC–anti-CD11b (M1/70), PE–anti-GR1 (RB6-8C5), FITC–anti-CD11c (N418), PE– or APC–anti-F4/80 (BM8), PE–anti-NK1.1 (PK136), PE–anti-CD49b (DX5), PE–anti-CD3e (145-2C11), FITC–anti-CD4 (GK1.5), FITC–anti-CD8a (53-6.7), and PE- and anti-CD19 (MB19-1; eBioscience and Biolegend; Table S2). Samples were analyzed with FACSCalibur (BD Biosciences), and data analysis was performed using FlowJo software (Tree Star). For intracellular cytokine staining, we freshly isolated tumors from polyI:C or PBS-injected mice at 1 h and incubated the cells in the presence of 10 μg/mL Brefeldin A for 3 h. Cells were fixed and stained with the combination of anti-CD45.2 Ab and anti-F4/80 Ab or anti-Gr1 Ab, followed by permeabilizing and staining with anti-TNF Ab using BD Cytofix/Cytoperm Kit (BD Biosciences).

Quantitative PCR Analysis. Tumor samples were cut into small pieces and homogenized with TRIzol Reagent (Invitrogen). Total RNA was isolated according to the manufacturer's instruction. Reverse transcription was performed using High-Capacity cDNA Reverse Transcription Kit (Applied Biosystems). Real-time PCR was performed with Power SYBR Green PCR Master Mix (Applied Biosystems) with a StepOne Real-Time PCR System (Applied Biosystems). Expression of the cytokine gene was normalized to the expression of *GAPDH*. We used primer pairs listed in Table S3. Data were analyzed by the ΔΔCt method.

ELISA and Cytokine Beads Assay. Tumor samples were cut into small pieces and homogenized with CelLytic MT Mammalian Tissue Lysis/Extraction Reagent (Sigma) supplemented with Complete Protease Inhibitor Mixture (Roche) on ice. Lysate was centrifuged to remove insoluble materials, and the supernatant was used for ELISA. Serum cytokine concentration was determined by ELISA or cytokine bead assays. Data were shown as TNF-α (pg) per weight of tumor (g).

Histochemistry and Immunohistochemistry. 3LL tumor was fixed with buffered 10% formalin overnight and embedded in paraffin wax, and sections 4 μm in thickness were stained with H&E. For immunohistochemistry, tumor was embedded in optimal cutting-temperature compound, and snap-frozen in liquid nitrogen. Cryosections 6 μm in thickness were air-dried for 60 min and fixed for 15 min with prechilled acetone and then incubated with FITC–anti-CD31 antibody (390; BioLegend). The sections were mounted in Prolong Gold Antifade Reagent with DAPI (Invitrogen). Images were obtained with a Leica LSM510 confocal laser-scanning microscope.

Tumor Challenge and PolyI:C Treatment. Mice were shaved at the back and injected s.c with 200 μL of 3×10^6 3LL cells in PBS(−). Tumor size was measured using a caliper. Tumor volume was calculated using the following formula: tumor volume (cm^3) = (long diameter) × (short diameter)^2 × 0.4. PolyI:C (250 μg/head) with no detectable LPS was injected i.p. as indicated. In some cases, polymixin B-treated polyI:C was used. When an average tumor volume of 0.5–0.8 cm^3 was reached, the treatment was started and repeated every 4 d.

Isolation of $F4/80^+$ Cells from Tumor. Tumors formed by 3LL cells were excised at 2 wk after transplantation and treated with 0.05 mg/mL Collagenase I (Sigma), 0.05 mg/mL Collagenase IV (Sigma), 0.025 mg/mL hyaluronidase (Sigma), and 0.01 mg/mL DNase I (Roche) in HBSS at 37 °C for 10 min. $F4/80^+$ cells were isolated by using biotinylated anti-F4/80 antibody (BM8) and Streptavidin MicroBeads (Miltenyi). We routinely prepared $F4/80^+$ cells at >90% purity from tumor.

1. Zitvogel L, et al. (1995) *Cancer immunotherapy of established tumors with IL-12. Effective delivery by genetically engineered fibroblasts. J Immunol* 155:1393–1403.
2. Masuda H, et al. (2002) High levels of RAE-1 isoforms on mouse tumor cell lines assessed by the anti-pan-Rae-1 polyclonal antibody confers tumor cell cytotoxicity on mouse NK cells. *Biochem Biophys Res Commun* 290:140–145.
3. Smyth MJ, et al. (2004) NKG2D recognition and perforin effector function mediate effective cytokine immunotherapy of cancer. *J Exp Med* 200:1325–1335.
4. Remels L, Fransen L, Huygen K, De Baetselier P (1990) Poly I:C activated macrophages are tumoricidal for TNF-α-resistant 3LL tumor cells. *J Immunol* 144:4477–4486.

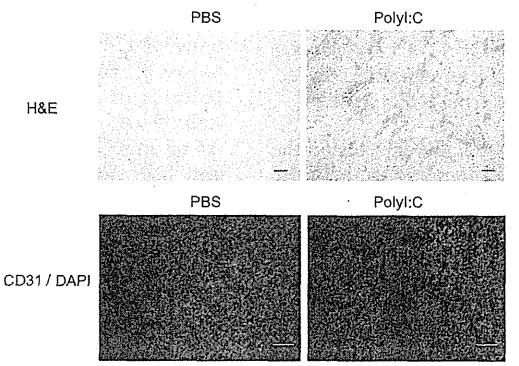

Fig. S1. Poly I:C induces hemorrhagic necrosis of tumor. 3LL tumor-bearing mice were i.p. injected with 200 μg poly I:C and tumors were isolated 12 h later. Formalin-fixed tumors stained with H&E (*Upper*) and frozen sections stained with anti-CD31 antibody and DAPI nuclear stain (*Lower*). Original magnification 10× for all panels. (Scale bars, 100 μm.) A representative experiment of three with similar outcomes is shown.

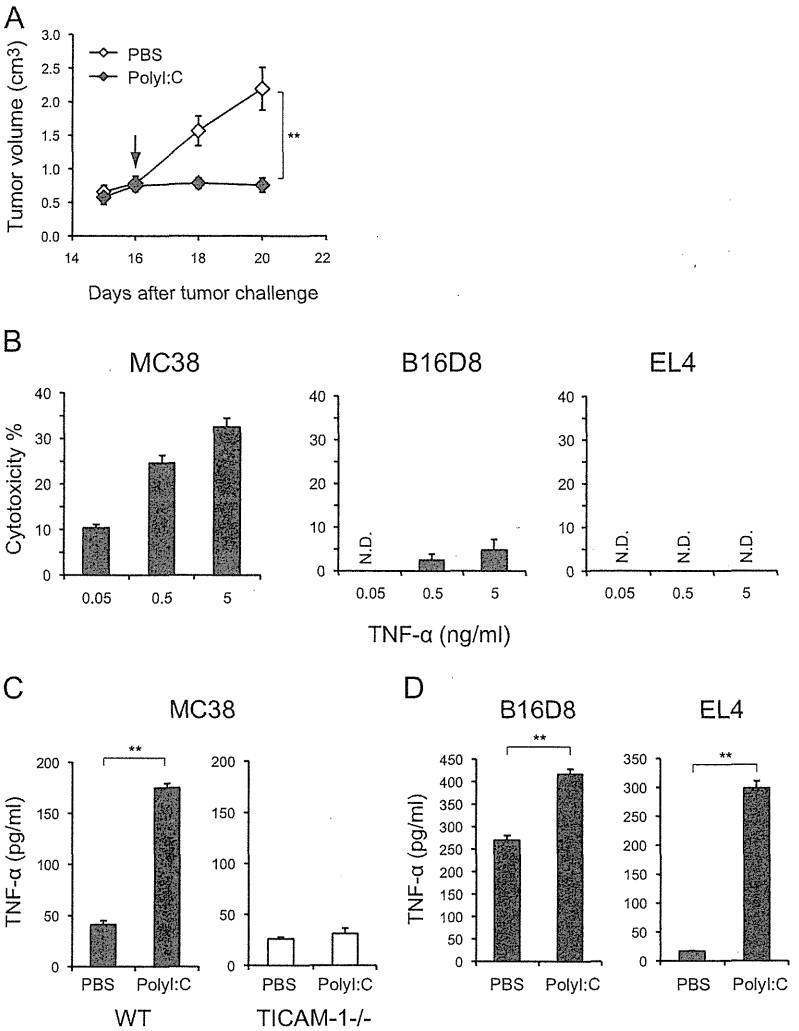

Fig. S2. Polyl:C induces TNF-α production by tumor-associated F4/80$^+$ Mfs in various types of tumor. (*A*) MC38 cells (1×10^5) were s.c implanted into C57BL/6 mice (day 0). Polyl:C (200 μg) was i.p. injected on day 16. Data are shown as tumor average size ± SE; $n = 3$–4 mice per group. (*B*) Sensitivity of MC38, B16D8, and EL4 cells to recombinant TNF-α. (*C* and *D*) MC38, B16D8, and EL4 tumor-bearing mice were i.p injected with 200 μg polyl:C. After 1 h, F4/80$^+$ cells were isolated from tumors and incubated for 24 h. TNF-α concentration in the conditioned medium was determined by ELISA; $n = 3$. Data are shown as average ± SD. N.D., not detected. A representative experiment of two with similar outcomes is shown.

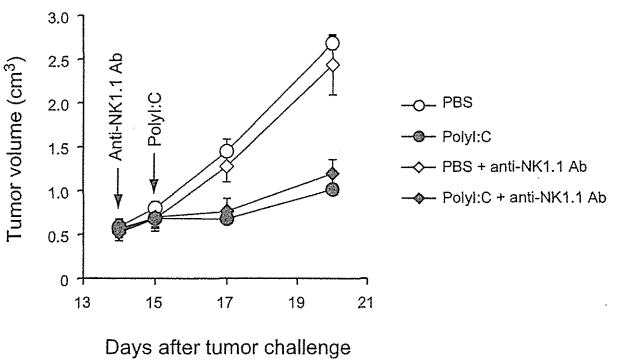

Fig. S3. NK cells are not essential for polyl:C-induced antitumor activity in vivo. 3LL tumor cells (3×10^6) were s.c transplanted into C57BL/6 mice (day 0). NK cells were depleted by injection of anti-NK1.1 antibody (PK136) into 3LL tumor-bearing mice on day 14. All doses of antibody and treatment regimens were determined in preliminary studies using the same lot of antibodies used for the experiments. Treatment was confirmed to deplete completely the desired cell populations for the entire duration of the study. Polyl:C (250 μg) was i.p injected on day 15 and the tumor volume was measured. Data shown are means ± SE, $n = 3$. A representative experiment of two with similar outcomes is shown.

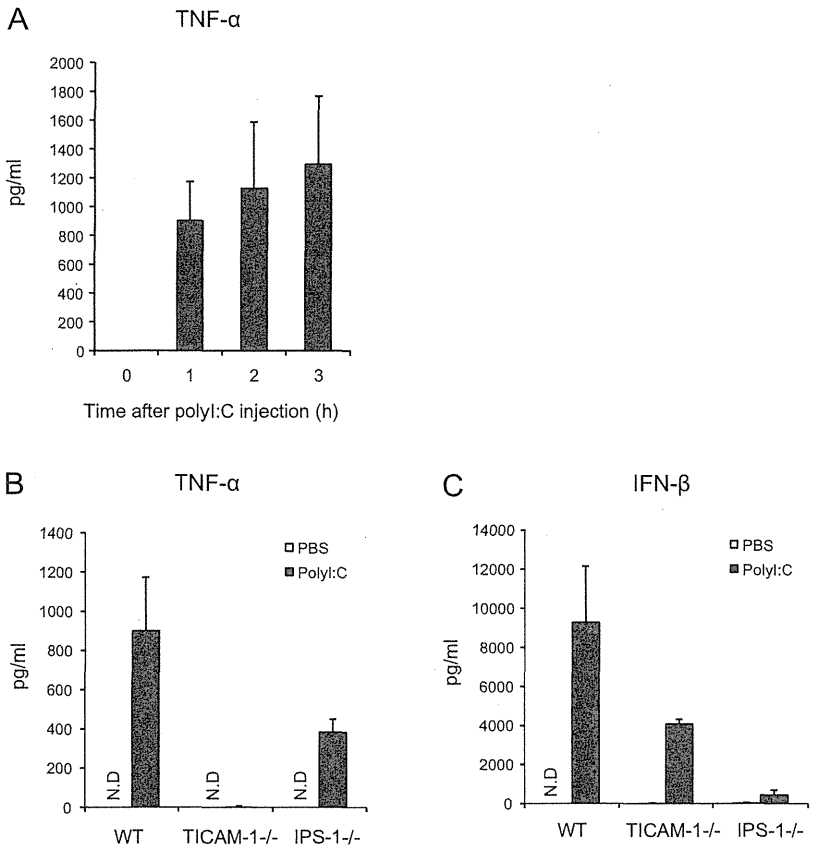

Fig. S4. Cytokine production in polyI:C-treated mouse. (*A*) WT mice were injected i.p with 200 μg polyI:C. After 0, 1, 2, and 3 h, TNF-α concentration in serum was determined by ELISA. (*B* and *C*) WT, TICAM-1$^{-/-}$, and IPS-1$^{-/-}$ mice were injected i.p with 200 μg polyI:C. After 1 h for TNF-α (*B*) and 4 h for IFN-β (*C*), serum cytokine levels were determined by ELISA. Data represents mean ± SD (n = 3). N.D., not detected. A representative experiment of three with similar outcomes is shown.

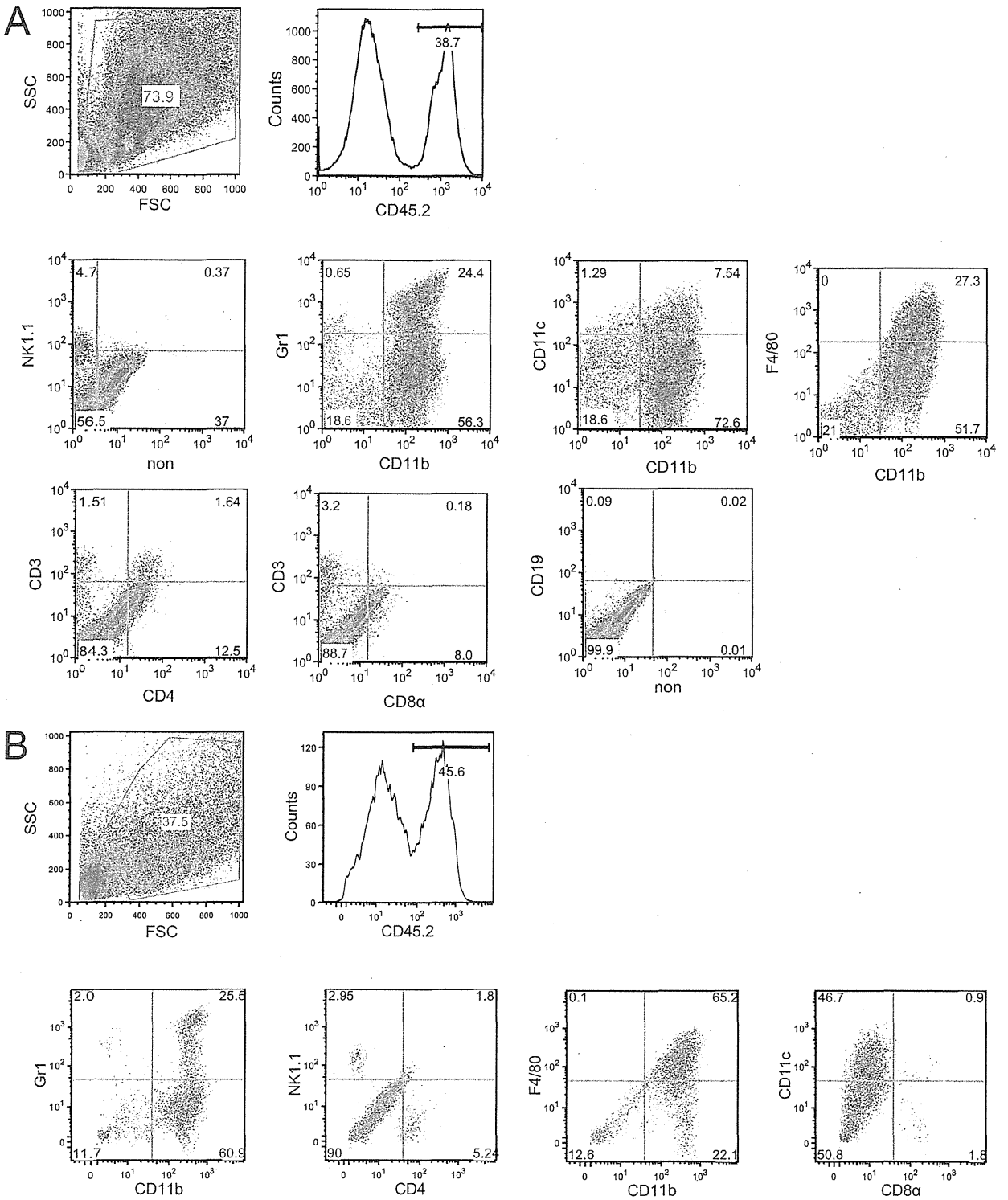

Fig. S5. Analysis of immune cells infiltrated into tumor. 3LL tumor cells (3×10^6) (*A*) or MC38 (1×10^6) (*B*) were transplanted s.c into B6 WT mice. After 2 wk, flow cytometric analysis was performed using freshly isolated whole tumor cell preparations in combination with staining of surface markers. CD45.2$^+$ cells were gated, and the expression of indicated surface markers was further analyzed. Numbers represent percentage of the gated and positive cells. A representative experiment of two with similar outcomes is shown. FSC, forward scatter; SSC, side scatter.

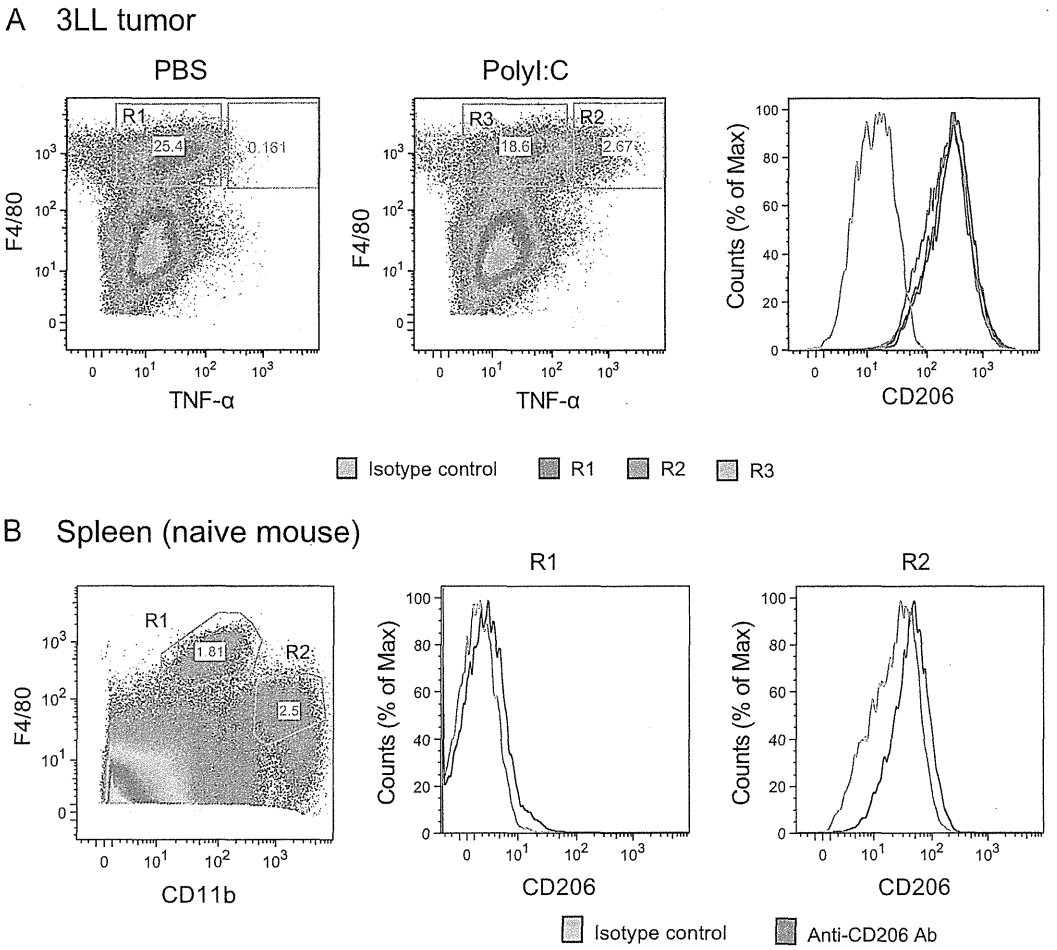

Fig. S6. Both TNF-α–producing and –nonproducing F4/80$^+$ macrophages in 3LL tumor of polyI:C-injected mouse express CD206 (macrophage mannose receptor). (*A*) 3LL tumor-bearing mice were injected i.p with 200 μg polyI:C. After 1 h, single-cell suspension of tumor was incubated in the presence of 10 μg/mL Brefeldin A for 3 h. Intracellular cytokine staining for TNF-α in CD45.2$^+$F4/80$^+$ cells was performed. R2, and R1 and R3 indicates TNF-α–producing and –nonproducing F4/80$^+$ cells, respectively. (*B*) CD206 expression in splenic F4/80$^+$CD11b$^+$ cells (R1 and R2) of naive mouse.

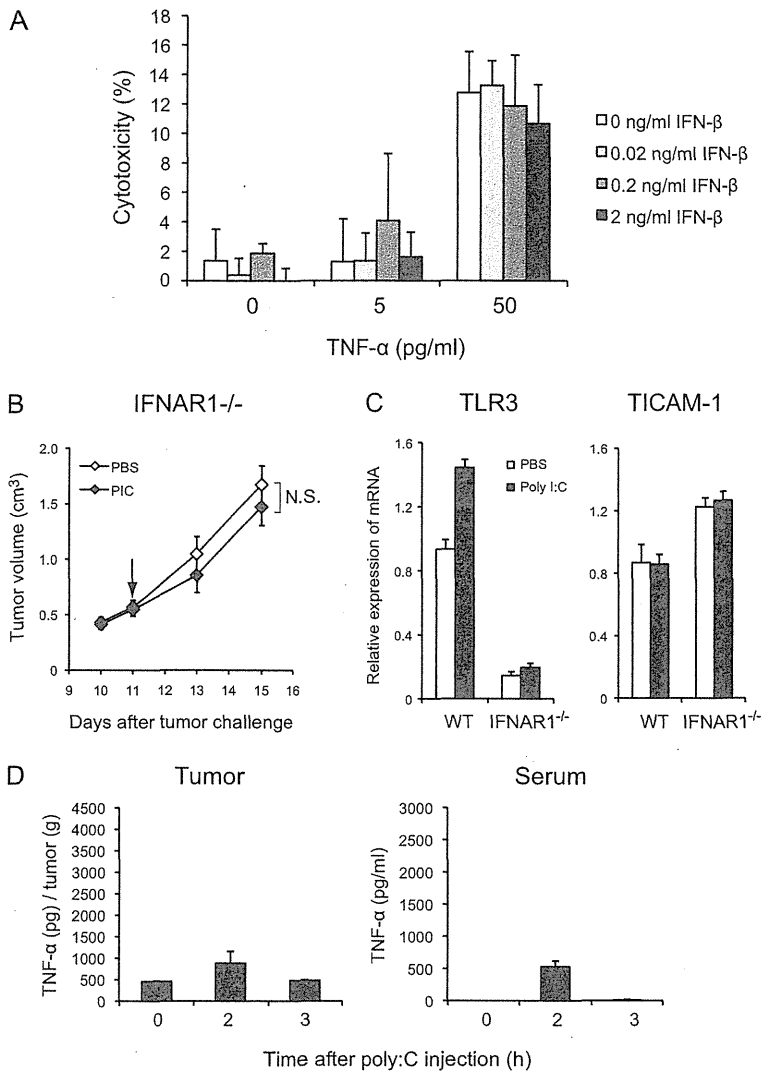

Fig. S7. Involvement of type I IFN signaling in 3LL tumor regression induced by polyI:C. (*A*) Effect of IFN-β on cytotoxic activity of TNF-α against 3LL tumor cells. 3LL cells were incubated in the presence of 0, 5, and 50 pg/mL recombinant mouse TNF-α in combination with 0, 0.02, 0.2, and 2 ng/mL recombinant mouse IFN-β. Cytotoxicity was determined by ^{51}Cr release assay. (*B*) Disabling polyI:C for 3LL tumor regression in IFN-α/β receptor $(IFNAR1)^{-/-}$ mice. PolyI:C was i.p injected on day 11; $n = 3–4$ mice per group. Data are shown as average ± SE. N.S., not significant. (*C*) Levels of the mRNA of TLR3 and TICAM-1 in 3LL tumor-associated $F4/80^{+}$ cells of WT or $IFNAR1^{-/-}$ mice. (*D*) TNF-α levels in tumor and serum in polyI:C-stimulated $IFNAR^{-/-}$ mice. Mice bearing 3LL tumors were i.p. injected with 200 μg polyI:C. Tumor (*Left*) and serum (*Right*) were collected at 0, 2, and 3 h after polyI:C injection, and TNF-α concentration was determined by ELISA. TNF-α level in tumor is presented as [TNF-α protein (pg)/tumor weight (g)].

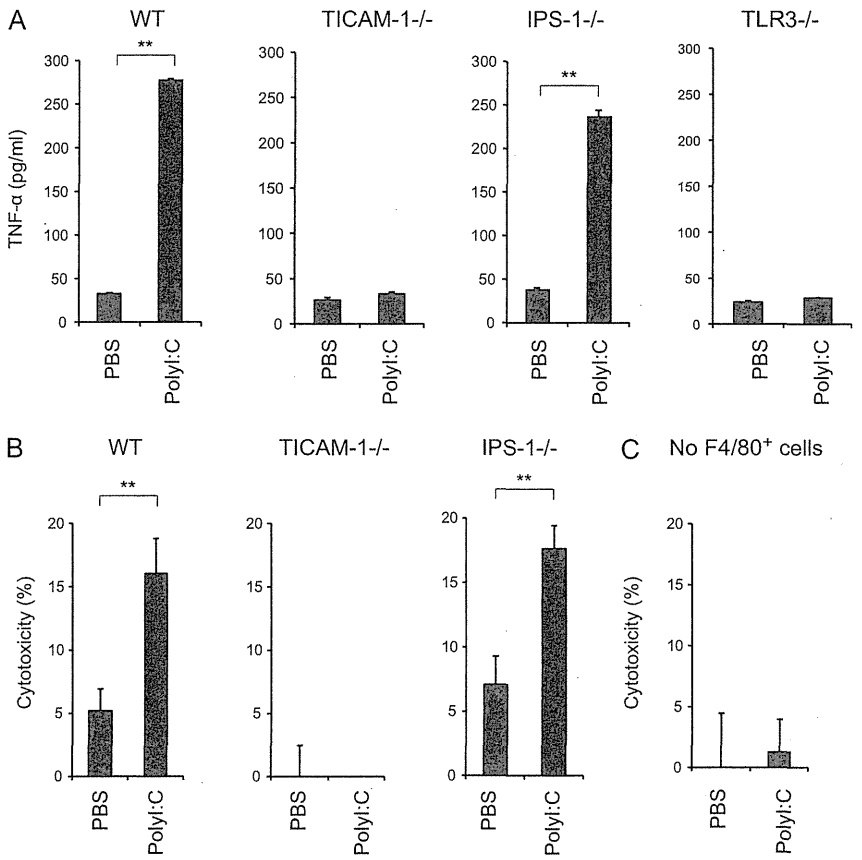

Fig. S8. In vitro polyI:C-stimulated F4/80$^+$ cells secrete TNF-α and have cytotoxic activity. (*A*) F4/80$^+$ cells isolated from 3LL tumor were stimulated with polyI:C (50 μg/mL) in vitro. After 24 h, the conditioned medium was collected and TNF-α concentration was determined by ELISA. (*B*) F4/80$^+$ cells isolated from tumor were mixed with ^{51}Cr-labeled 3LL tumor cells in the presence or absence of polyI:C (50 μg/mL). After 20 h, radioactivity of the conditioned medium was measured. E/T = 10. (*C*) ^{51}Cr-labeled 3LL tumor cells were incubated for 20 h in the presence or absence of polyI:C (50 μg/mL); $n = 3$. Data are shown as average ± SD. $^{**}P < 0.001$. A representative experiment of three with similar outcomes is shown.

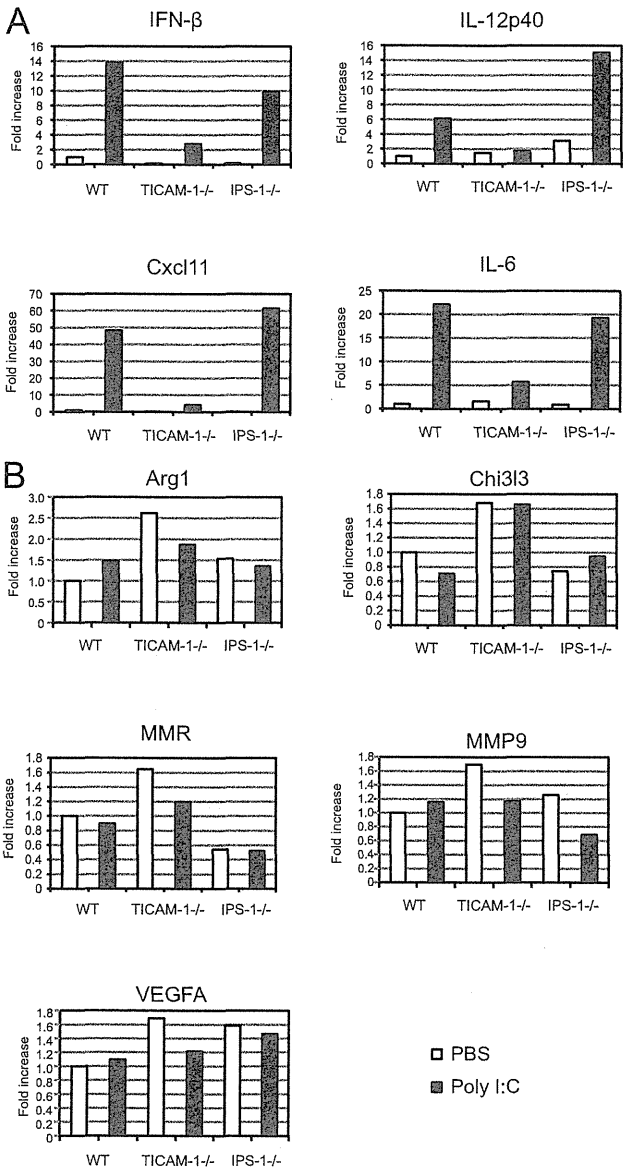

Fig. S9. Poly I:C induces the expression of M1 but not M2 macrophage-associated genes in tumor-infiltrated F4/80$^+$ cells through the TICAM-1 pathway. 3LL tumor-bearing mice were i.p injected with 200 μg poly I:C. After 3 h, tumors pooled from two mice treated with poly I:C or PBS were mixed. F4/80$^+$ cells were isolated from the mixed tumor, and the expression of (*A*) M1- and (*B*) M2-related genes was analyzed. A representative experiment of two with similar outcomes is shown.

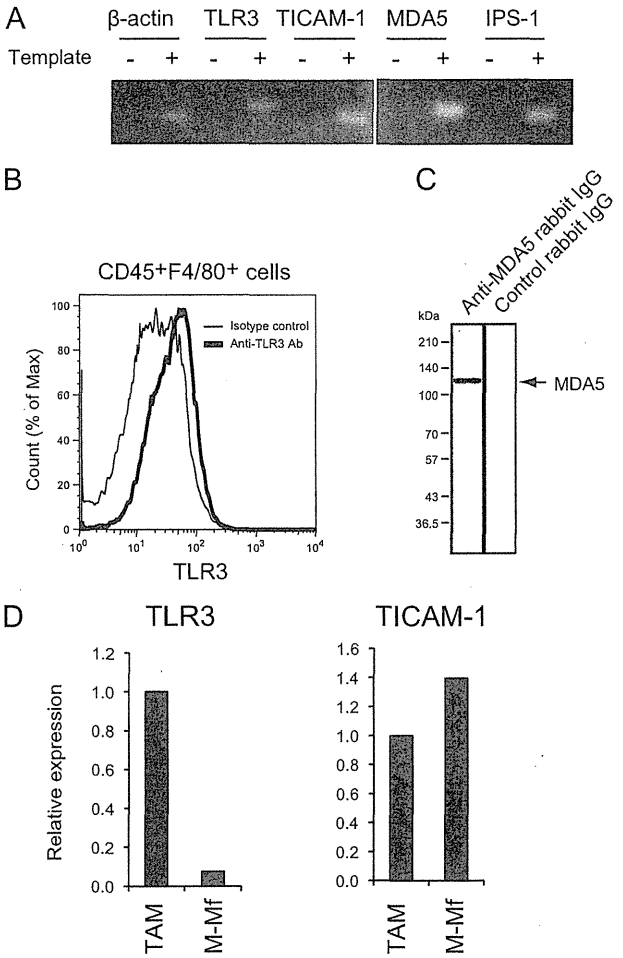

Fig. S10. Expression of TLR3 and MDA5 in 3LL tumor-associated F4/80$^+$ cells. (*A*) mRNA expression of TLR3, TICAM-1, MDA5, and IPS-1 in 3LL tumor-associated F4/80$^+$ cells. Total RNA (1 μg) of F4/80$^+$ cells isolated from 3LL tumor was used as a template for RT-PCR analysis. (*B*) Single-cell suspension of 3LL tumor was stained with FITC-labeled anti-CD45 and PE-labeled anti-F4/80 antibody, followed by intracellular staining with Alexa 647-labeled anti-TLR3 antibody (11F8) or isotype control antibody (rat IgG2a). CD45$^+$F4/80$^+$ cells are shown. (*C*) Cytoplasmic extract of F4/80$^+$ cells was subjected to SDS/PAGE and immunoblotted with rabbit anti-MDA5 antibody or control IgG purified from rabbit serum. (*D*) mRNA expression of TLR3 and TICAM-1 in F4/80$^+$ tumor-associated macrophages (TAM) and macrophage colony-stimulating factor-induced bone marrow-derived macrophages (M-Mf).

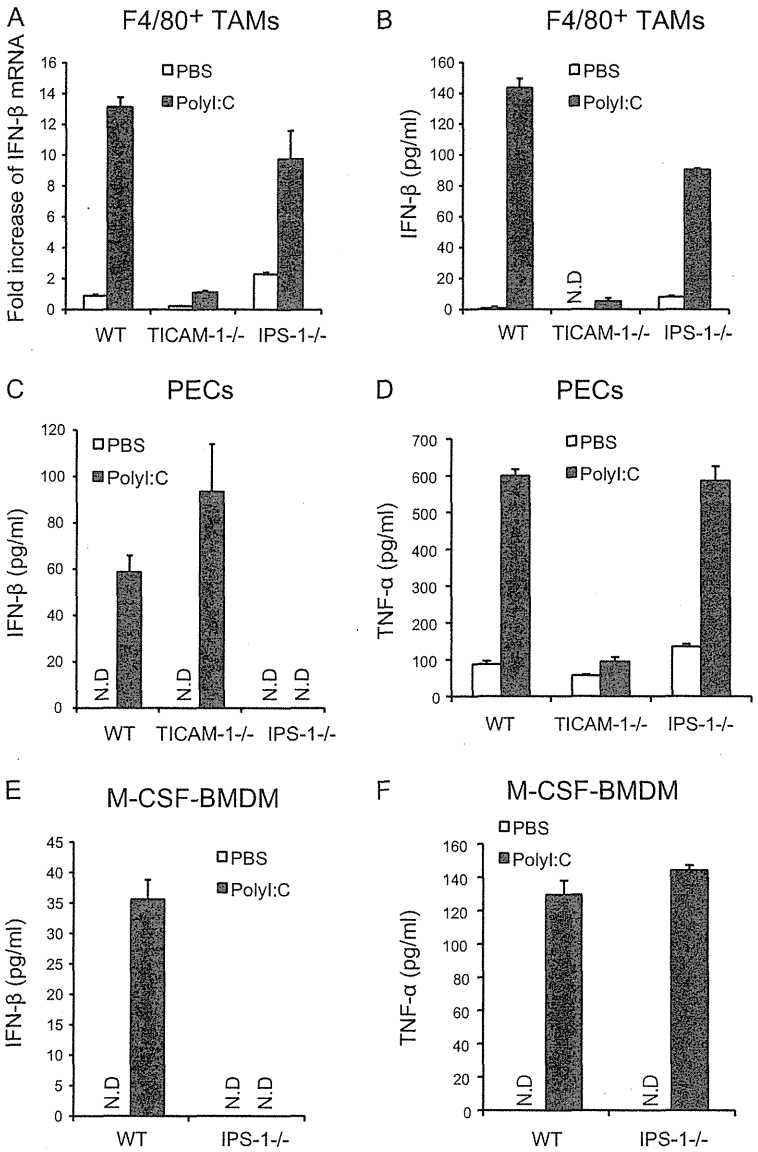

Fig. S11. In vitro stimulation with polyI:C increases the production of IFN-β and TNF-α by Mfs. (*A* and *B*) F4/80$^+$ cells were isolated from 3LL tumor implanted in WT, TICAM-1$^{-/-}$, and IPS-1$^{-/-}$ mice and stimulated with 50 μg/mL polyI:C. After 4 h, cells were harvested and IFN-β mRNA expression was analyzed by quantitative PCR analysis (*A*). After 20 h, IFN-β concentration in culture supernatant was determined by ELISA (*B*). (*C* and *D*) Peritoneal exudate cells (PECs) isolated from WT, TICAM-1$^{-/-}$, and IPS-1$^{-/-}$ mouse were stimulated with 50 μg/mL polyI:C for 20 h. The concentrations of IFN-β (*C*) and TNF-α (*D*) in culture supernatant were determined by ELISA. (*E* and *F*) Macrophage colony-stimulating factor (M-CSF)-induced bone marrow-derived macrophages (BMDM) were prepared from WT and IPS-1$^{-/-}$ mouse and cultured in the presence of 30% L929 supernatant containing M-CSF. After 6 d, adherent cells were harvested and stimulated with 50 μg/mL polyI:C for 20 h. The concentrations of IFN-β (*E*) and TNF-α (*F*) in culture supernatant were determined by ELISA. Data are shown as mean ± SD ($n = 3$). N.D., not detected. A representative experiment of two with similar outcomes is shown.

Table S1. Expression of various markers on 3LL and MC38 tumor cells

Surface marker	3LL	MC38
H2-K^b	–	++
H2-D^b	±	++
RAE1	++	Not determined
CD45	–	–

Expression of surface markers was analyzed by flow cytometry. Expression was evaluated by mean fluorescence shift: –, ~0.99 ; ±, 1~10 ; +, 11~100 ; ++, 101~.

Table S2. RT-PCR primers used in this study

	Forward primer (5′–3′)	Reverse primer (5′–3′)
IFN-β	CCAGCTCCAAGAAAGGACGA	CGCCCTGTAGGTGAGGTTGAT
IL-12p40	AATGTCTGCGTGCAAGCTCA	ATGCCCACTTGCTGCATGA
IL-6	GTGCATCATCGTTGTTCATACAATC	CTGGGAAATCGTGGAAATGAG
TNF-α	AGGGATGAGAAGTTCCCAAATG	GCTTGTCACTCGAATTTTGAGAAG
IL-1β	TGACGGACCCCAAAAGATGA	TGCTGCTGCGAGATTTGAAG
IL-10	GGCGCTGTCATCGATTTCTC	TGCTCCACTGCCTTGCTCTTA
Cxcl11	GGCTGCGACAAAGTTGAAGTGA	TCCTGGCACAGAGTTCTTATTGGAG
IRF4	AGCCCAGCAGGTTCATAACTACA	CCTCGTGGGCCAAACGT
IRF5	GGTCAACGGGGAAAAGAAACT	CATCCACCCCTTCAGTGTACT
Jmjd3	CGAGTGGTTCGCGGTACAT	GAAGCGGTAAACAGGAATATTGGA
Arg1	GGAATCTGCATGGGCAACCTGTGT	AGGGTCTACGTCTCGCAAGCCA
MMP9	CAAGTGGGACCATCATAACATCA	GATCATGTCTCGCGGCAAGT
VEGFA	GACATCTTCCAGGAGTACC	TGCTGTAGGAAGCTCATCT
Chi3l3	TCACTTACACACATGAGCAAGAC	CGGTTCTGAGGAGTAGAGACCA
Mrc1	CTCTGTTCAGCTATTGGACGC	CGGAATTTCTGGGATTCAGCTTC
Retnla	CCAATCCAGCTAACTATCCCTCC	ACCCAGTAGCAGTCATCCCA
GAPDH	GCCTGGAGAAACCTGCCA	CCCTCAGATGCCTGCTTCA

Table S3. Expression of surface markers on tumor-infiltrated F4/80$^+$ cells

Marker	Expression*
I-Ab	+
H2-D^b	+
H2-K^b	+
CD80	++
CD86	++
CD40	±
CD11c	±
CD3	−
CD4	−
CD8α	−
Gr1	+
B220	+
CD11b	+++
CD206 (MMR)	++

*Expression was evaluated by mean fluorescence shift: −, ~0.99 ; ±, 1 ~10 ; +, 11 ~100 ; ++, 101 ~1,000 ; +++, 1,001~.

Microbiol Immunol 2012; **56**: 1–9
doi:10.1111/j.1348-0421.2011.00403.x

REVIEW

In vitro models for analysis of the hepatitis C virus life cycle

Hussein H. Aly[1,2], Kunitada Shimotohno[3], Makoto Hijikata[4] and Tsukasa Seya[1]

[1]Department of Microbiology and Immunology, Hokkaido University Graduate School of Medicine, Kita-15, Nishi-7, Kita-ku, [2]Laboratory of Viral Hepatitis and Host Defense, Hokkaido University Creative Research Institution, Kita-22, Nishi-7, Kita-ku, Sapporo 060-8638, [3]Research Institute, Chiba Institute of Technology, Narashino 275-0016, Chiba and [4]Department of Virology, Virus Research Institute, Kyoto University, Kyoto 606-8507, Japan

ABSTRACT

Chronic hepatitis C virus (HCV) infection affects approximately 170 million people worldwide. HCV infection is a major global health problem as it can be complicated with liver cirrhosis and hepatocellular carcinoma. So far, there is no vaccine available and the non-specific, interferon (IFN)-based treatments now in use have significant side-effects and are frequently ineffective, as only approximately 50% of treated patients with genotypes 1 and 4 demonstrate HCV clearance. The lack of suitable *in vitro* and *in vivo* models for the analysis of HCV infection has hampered elucidation of the HCV life cycle and the development of both protective and therapeutic strategies against HCV infection. The present review focuses on the progress made towards the establishment of such models.

Key words hepatitis C virus, HuH-7 cell, knockout mice, type I interferon.

Chronic HCV infection is a major cause of mortality and morbidity throughout the world, infecting approximately 3.1% of the world's population (1). Only a fraction of acutely infected individuals are able to clear the infection spontaneously, whereas approximately 80% of infected individuals develop a chronic infection (2, 3). Patients with chronic HCV are at increased risk for developing liver fibrosis, cirrhosis, and/or hepatocellular carcinoma. Currently, these long-term complications of chronic HCV infection are the leading indication for liver transplantation (4, 5). Because of the high incidence of new infections by blood transfusions in the 1980s before the discovery of the virus, and because morbidity associated with chronic HCV infection generally takes decades to develop, it is expected that the burden of disease in the near future will rise dramatically.

HCV is an enveloped flavivirus, with a positive-stranded RNA genome of approximately 9600 nucleotides. The coding region is flanked by 5′ and 3′ non-coding regions, which are important for the initiation of translation and regulation of genomic duplication, respectively. The coding region itself is composed of a single open reading frame, which encodes a polyprotein precursor of approximately 3000 amino acids. This polyprotein is cleaved by host and viral proteases into structural and NS proteins (Fig. 1). Replication of the HCV genome involves the synthesis of a full-length negative-stranded RNA intermediate, which in turn provides a template for the de novo production of positive-stranded RNA. Both these synthesis steps are mediated by the viral RNA-dependent RNA polymerase NS5B (6–8). NS5B lacks proofreading abilities, and this leads to a high mutation rate and the

Correspondence
Hussein H. Aly, Department of Microbiology and Immunology, Graduate School of Medicine, Hokkaido University, Kita-ku, Sapporo 060-8638, Japan.
Tel: +81 11 706 5073; fax: +81 11 706 5056; email: ahussein@med.hokudai.ac.jp

Received 8 September 2011; revised 23 October 2011; accepted 3 November 2011.

List of Abbreviations: 3-D, three-dimensional; 3-D/HF, three-dimensional hollow fiber system; bbHCV, blood borne hepatitis C virus; HCV, hepatitis C virus; HPV/E6E7, human papilloma virus E6/E7 genes; IFN, interferon; IFNAR, interferon A receptor; IRES, internal ribosome entry site; ko, knockout; MDA-5, melanoma differentiation associated gene 5; MEF, mouse embryo fibroblasts; mir199, micro RNA 199; NS proteins, non-structural proteins; PPAR, peroxisome proliferator-activated receptor; RFB, radial flow bioreactor; RIG-I, retinoic acid-inducible gene I; TLR, Toll-like receptor; uPA, urokinase plasminogen activator.

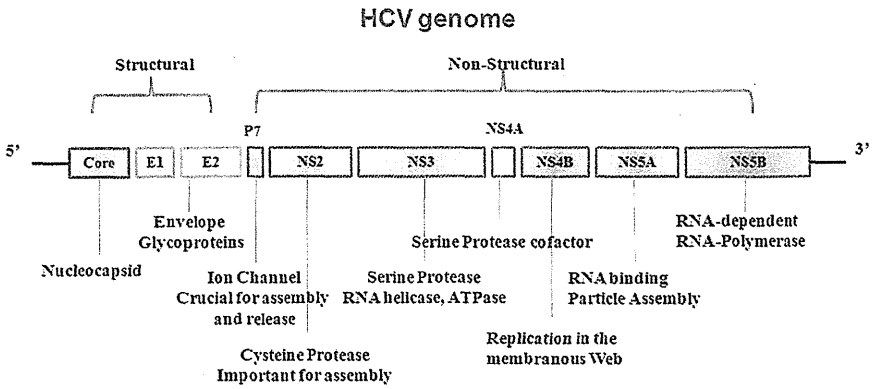

Fig. 1. Genomic structure of HCV. Genomic organization of wild-type HCV. The HCV-RNA genome consists of a major open reading frame, encoding a single polyprotein, and an alternative reading frame encoding F-proteins with unknown functions. The cleavage of the polyprotein by viral and host cell proteases gives rise to the mature structural (core, envelope proteins E1 and E2, and p7) and NS viral proteins (NS2 through NS5B). The putative activities and functions of viral proteins are indicated. The IRES located in the 5′ non-coding region initiates ribosome binding and translation. Both the 5′ and 3′ non-coding regions are essential for viral RNA replication involving the RNA-dependent RNA polymerase NS5B. NTPase, nucleotide triphosphatase.

generation of numerous quasispecies. HCV isolates can be classified into seven major genotypes, which vary in sequence by more than 30%. In addition to the distinct prevalence and global spread of the virus, the genotype is an important factor determining disease progression and responses to antiviral therapy (9).

Currently, the only licensed treatment for HCV is the combination of (pegylated)-interferon-alpha (IFN-α) and ribavirin. Although the success rate of treatment has improved substantially, standard therapy is not effective in all patients. Moreover, severe adverse effects and high costs limit the compliance and global application of this treatment. The development of prophylaxis and novel therapeutics to treat HCV infection has been hampered by the lack of suitable *in vitro* and *in vivo* culture systems. In this review, we describe the development of *in vitro* culture systems for HCV.

Tissue culture-adapted HCV (sub-)genomic replicons

Dr Bartenschlager's group was the first to establish a convenient reproducible *in vitro* cell culture system for the study of HCV replication (10). They created antibiotic-resistant HCV genomes to select replication-competent viral clones by conveying antibiotic resistance to cells. This was achieved by replacing the structural protein-coding sequences, as well as p7 of the consensus genome Con1, by the neomycin resistance gene. In addition, a second IRES was introduced to promote translation of the non-structural protein-coding sequences important for viral replication (Fig. 2). Upon transfection of these so-called subgenomic replicons in specific cell lines, drug-resistant cell colonies were isolated in which high levels of viral replication occurred. Subsequent analysis confirmed that these HCV replicons indeed were capable of self-amplification through synthesis of a negative-strand replication intermediate, and could be stably propagated in cell culture for many years (10, 11).

HCV replication was supported by several cell types such as HuH6 (12), HepG2 (13), Li23 (14), and 293 cells (15), with the human hepatoma cell line HuH-7 being the most permissive (16). Interestingly, removal of replicon RNA from these cell clones by treatment with type 1 IFN rendered the cells more permissive to reintroduction of replicons, resulting in higher replication rates. Examples of these highly permissive cells are HuH-7.5 and HuH-7-Lunet cells (16, 17). The efficient replication in the replicon systems was found to depend on tissue-culture-adaptive mutations. Introduction of these specific mutations in the wild-type consensus sequence significantly enhanced viral replication *in vitro* (18–22). Mutational hot spots were found clustered primarily in the NS3, NS4B, and NS5A regions. The mechanisms behind the enhanced replication caused by these tissue-culture-adaptive mutations are still largely unknown, and the interesting fact that these mutations are not commonly found in patients suggests that these may have a toll on the viral fitness.

HCV replicons have proven to be extremely valuable for studies on the process of HCV replication, as well as for testing novel antiviral compounds that specifically target the protease activity of NS3 or the polymerase activity of NS5 (23).

Cell culture-derived infectious HCV

Studies using HCV replicons have provided detailed knowledge on the mechanisms of replication of HCV.

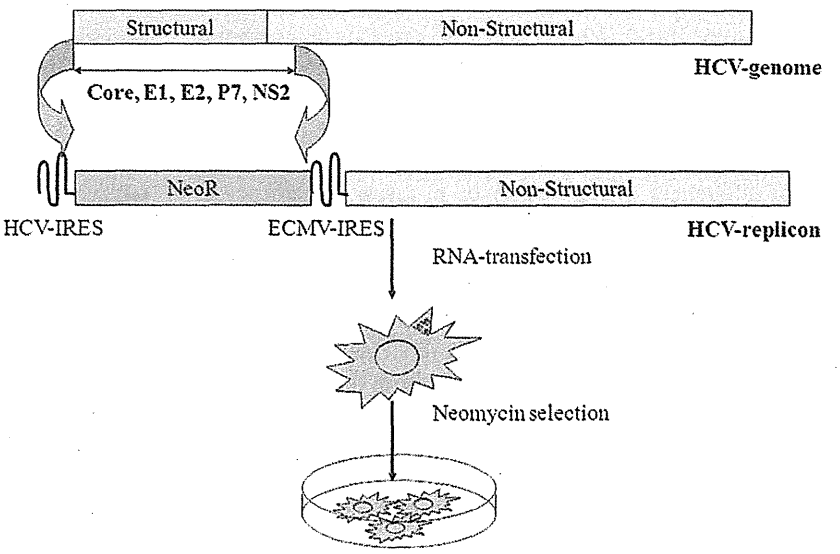

Fig. 2. HCV replicon system. The structural sequences (C, E1, E2, and p7) together with NS2 were replaced by a neomycin antibiotic-resistance gene, and an ECMV-IRES was introduced to drive translation of the remaining non-structural proteins. Neomycin selection of these double cistron (bicistronic) replicons in the hepatoma cell line Huh7 resulted in high-level HCV-RNA replication, depending on the gain of so-called 'tissue-culture' adaptive mutations mostly confined to the NS3, NS4B, and NS5A regions.

However, an apparent shortcoming of these models was that stable cell clones containing self-replicating replicons and expressing all viral proteins remained unable to release infectious HCV particles. The inability to secrete viral particles may be the consequence of adaptive mutations, which are needed to enhance viral replication rates, but at the same time may block viral assembly. Indeed, replicons without adaptive mutations show very low replication rates (16, 24). A different situation emerged when the first genotype 2a consensus genome was established (25, 26).

A subgenomic replicon constructed from a clone called JFH-1, isolated from a Japanese patient with fulminant hepatitis C, replicated up to 20-fold higher in HuH-7 cells as compared to Con1 replicons, and did not require adaptive mutations for efficient replication *in vitro* (26). Transfection of HuH-7 and HuH-7.5.1 cells with the *in vitro*-transcribed full-length JFH-1 genome or a recombinant chimeric genome with another genotype 2a isolate, J6, resulted in the secretion of viral particles that were infectious in cultured cells (Fig. 3), in chimeric mice, and in chimpanzees (27–29).

The infectivity of cells could be neutralized with antibodies against the HCV entry receptor CD81, antibodies against E2, or immunoglobulins from chronically infected patients. Importantly, the replication of cell-cultured HCV in this system was inhibited by IFN-α as well as by several HCV-specific antiviral compounds (29). Since 2005, chimeric JFH-1-based genomes have been constructed of all seven known HCV genotypes. Similar to the J6-JFH-1 chimera, in these so-called intergenotypic recombinants, the structural genes (core, E1, and E2), p7, and NS2 of JFH-1 were replaced by genotype-specific sequences which often resulted in lower infectious virion production than

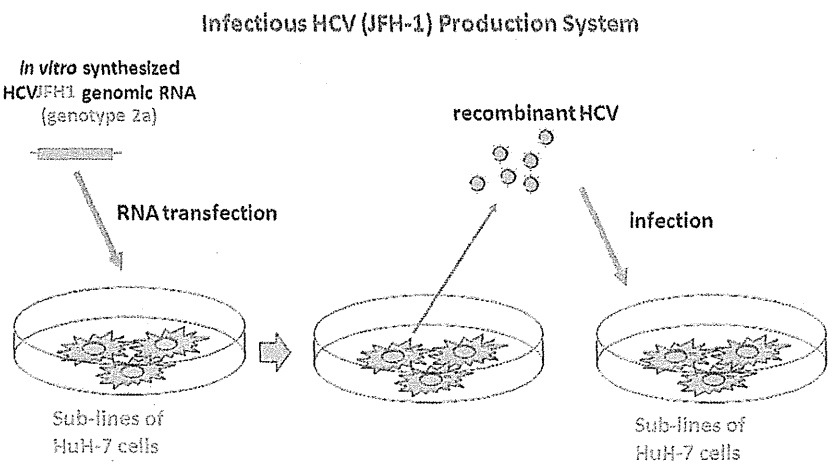

Fig. 3. JFH1 infectious system. Full-length JFH1-RNA is transcribed *in vitro*, and transfected to HuH-7-derived cell lines. JFH1 replicates in these cells, and produce infectious virions in the medium. The medium is collected, concentrated, and used to infect naive cells. Hence, the entire HCV life cycle was reproduced for the first time *in vitro*.